

# The Berezinskii-Kosterlitz-Thouless phase transition for the dilute planar rotator model on a triangular lattice

Yun-Zhou Sun\* and Lin Yi

*Department of Physics, Huazhong University of Science and Technology, Wuhan City, Hubei Province, 430074, China*

G. M. Wysin†

*Department of Physics, Kansas State University, Manhattan, KS 66506*

(Dated: 27 Aug, 2008)

The Berezinskii-Kosterlitz-Thouless phase transition for the dilute planar rotator model on a triangular lattice is studied by using a hybrid Monte Carlo method. The phase transition temperatures for different nonmagnetic impurity densities are obtained by three approaches: finite-size scaling of plane magnetic susceptibility, helicity modulus and Binder's fourth cumulant. It is found that the phase transition temperature decreases with increasing impurity density  $\rho$  and the BKT phase transition vanishes when the magnetic occupancy falls to the site percolation threshold:  $1 - \rho_c = p_c = 0.5$ .

PACS numbers: 07.05.Tp;21.60.Ka;05.10.Ln;75.10.Hk.

## I. INTRODUCTION

It is well known that the Berezinskii-Kosterlitz-Thouless (BKT) phase transition [1-2] caused by the unbinding of vortex-antivortex pairs is found to be common in two-dimensional ferromagnetic spin models, such as the planar rotator model, XY model and easy-plane Heisenberg model. Recently, the study of nonmagnetic impurities in these spin models has been the subject of much interest [3-7]. It is found that the BKT phase transition temperature decreases with increasing nonmagnetic impurity density  $\rho$ . However, a Metropolis algorithm Monte Carlo (MC) simulation [3] of the planar rotator model on a square lattice showed that the phase transition temperature  $T_C$  falls to zero for a magnetic occupation density  $\rho_{mag} = 1 - \rho$  above the site percolation limit  $p_c \approx 0.59$  on a square lattice. This phenomenon was also found in the dilute system of Josephson junctions [8]. These results were somewhat surprising, because they suggested that a mechanism besides the disordered (or disconnected) geometry of the impurity-occupied lattice was responsible for permanently leaving the magnetic system in a high-temperature disordered phase. On the other hand, through extensive hybrid MC simulation, Wysin *et al.* [6] found that the phase transition temperature drops to zero at  $\rho_{mag} \approx 0.59$ , the site percolation limit, where there is no more percolating cluster of spins. The disorder due to impurities, especially near the percolation limit, greatly increases fluctuations in the Monte Carlo, making hybrid schemes that include cluster and over-relaxation updates a necessity for precise results. This is counterintuitive, because one might naively expect that the weaker connectivity of the lattice

near the percolation limit should make the calculations easier. The problem is interesting, however, because just as the impurity concentration is getting near that limit that causes  $T_C$  to fall to zero, and the lattice is less and less connected, the correlation length is still diverging, causing all the usual problems that MC faces near a critical point.

The previous works were all focused on the spin system for the square lattice, but of course, there is also a BKT phase transition in the planar rotator model on the triangular lattice. The site percolation threshold of a triangular lattice is  $p_c = 0.5$  [9]. On a triangular lattice, cluster MC simulation of the pure system shows that the percolation temperature, defined as the temperature at which spanning clusters start to appear in a large system, equals the BKT phase transition temperature for the planar rotator model [10]. Therefore, the study of the BKT phase transition for the *dilute* planar rotator model on a triangular lattice is also interesting as a comparison to the square lattice. The main question to be answered is whether the BKT transition temperature falls to zero when the magnetic occupation density equals the site percolation limit, or whether this happens at an occupation density *higher* than the percolation limit. We carry this out here using a hybrid MC simulation that includes over-relaxation and cluster moves, which are important especially when the system is near the percolation threshold, where Metropolis single spin moves become inefficient.

## II. METHOD AND RESULTS

The Hamiltonian of the dilute planar rotator spin model is considered as [3, 6]

$$H = -J \sum_{\langle i,j \rangle} \sigma_i \sigma_j \vec{S}_i \cdot \vec{S}_j = -J \sum_{\langle i,j \rangle} \sigma_i \sigma_j \cos(\theta_i - \theta_j). \quad (1)$$

\*Electronic address: syz1979@163.com

†Electronic address: wysin@phys.ksu.edu; URL: <http://www.phys.ksu.edu/personal/wysin>

Here  $J > 0$  is the ferromagnetic coupling constant,  $\theta_i$  are the angular coordinates of two spin components  $\vec{S}_i = (S_i^x, S_i^y) = (\cos \theta_i, \sin \theta_i)$ , and  $\langle i, j \rangle$  indicates the nearest neighbor sites.  $\sigma$  is taken to be 1 or 0 depending on whether the site is occupied or not. A hybrid MC approach, including Metropolis algorithm [11] and over-relaxation algorithm [12,13] combined with Wolff single-cluster algorithm [14], proved to be very efficient for the model defined by equation (1) on a square lattice [6]. We apply this approach to this model on a triangular lattice.

The processes used in the hybrid MC scheme work as follows. In a Metropolis single spin update, one spin is selected randomly from total spins. The new candidate spin, obtained by a small increment to this spin in a random direction, is renormalized to unit length. Then the energy difference is obtained according to equation (1). The new spin is accepted or not according to a standard Metropolis judgement. An over-relaxation update reflects a spin selected randomly across the effective potential of its nearest neighbors, defined as  $\vec{B}_j = J \sum_j \sigma_j \vec{S}_j$ ,

with the reflection effected by  $\vec{S}_i \rightarrow 2 \frac{\vec{S}_i \cdot \vec{B}_j}{\|\vec{B}_j\|^2} \vec{B}_j - \vec{S}_i$ . This algorithm is non-ergodic and it must be mixed with other updates to achieve ergodicity. The Wolff cluster algorithm is similar to the application to a pure system, except that spins at vacant sites are set to zero length. The Over-relaxation and Wolff cluster algorithms generally reduce autocorrelations better than Metropolis single spin updates, especially at low temperatures where the spin components tend to freeze.

From an initial spin configuration by randomly occupying sites with probability  $1 - \rho$ , the simulation is performed with periodic boundary conditions for system size  $N = L^2$ , where the size of lattice is considered as  $L = 20, 30, 40, 60$ , and  $80$ . Then the number of magnetically occupied sites is  $N_{mag} = N(1 - \rho)$ . A hybrid MC step consists of one Wolff update of planar components of the spins followed by one Metropolis update and four over-relaxation updates, which change the configuration but keep the energy unchanged. For each algorithm of our scheme, one update is defined as attempting  $N_{mag}$  spin moves. During the simulation,  $1 \times 10^4$  MC steps are used for equilibration and about  $4 \times 10^5$  MC steps are used to get thermal averages at each temperature. To avoid correlations, measurements are taken every  $2 \sim 6$  MC steps. We used three different methods described in Ref. [6] to get the phase transition temperature  $T_C$ . As the MC proceeds, some thermodynamics are observed. For adequately sized systems, and small enough impurity density, averaging over different placements of the impurities makes little difference in the averages [6]. Therefore, we did not average over different placements of impurities for large sizes when  $\rho \leq 0.3$ . While the presence of impurities tends to amplify finite size effects, for large enough systems the fluctuations due to impurity disorder will become averaged out [6], and averages over impurity disorder become less necessary with

increasing  $L$ . Therefore, the focus is on the temperature dependence of thermal averages especially for the larger systems. Also, in the scaling with system size (such as for the susceptibility), the fluctuations (error bars) caused by impurity disorder should diminish rapidly with increasing  $L$ .

According to the magnetization  $\vec{M} = (M_x, M_y) = \sum_i \sigma_i \vec{S}_i$ , the susceptibility and susceptibility components are given by

$$\chi = [\langle (M)^2 \rangle - \langle M \rangle^2] / N_{mag} k_B T, \quad (2)$$

$$\chi^\alpha = [\langle M_\alpha^2 \rangle - \langle M_\alpha \rangle^2] / N_{mag} k_B T, \quad (3)$$

where  $k_B$  is the Boltzmann constant. With the average of  $\chi^x$  and  $\chi^y$ , the in-plane susceptibility is obtained

$$\chi' = (\chi^x + \chi^y) / 2. \quad (4)$$

The Binder fourth order cumulant is also defined via the usual relation [14]

$$U_L = 1 - \frac{\langle M^4 \rangle}{3 \langle M^2 \rangle^2}. \quad (5)$$

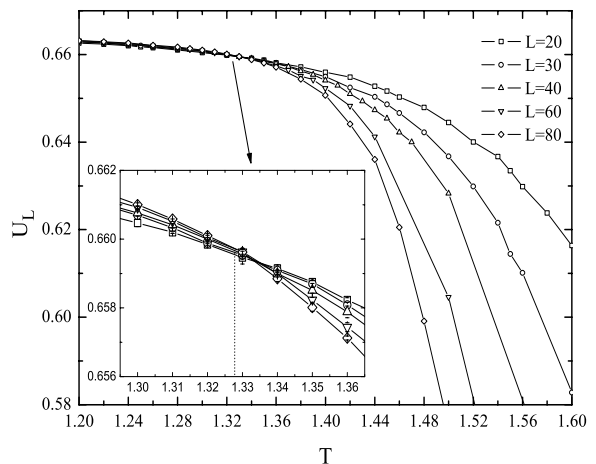


FIG. 1: Application of Binder's fourth order cumulant to estimate the phase transition temperature for several lattice sizes at  $\rho = 0.05$ . The inset shows the view near the estimated critical temperature.

In the figures, the error bars that are not visible indicate the statistical errors are smaller than the symbols. For convenience, temperatures are measured in units of the exchange constant,  $J$ .

Binder's fourth order cumulant  $U_L$  is used to estimate the location of  $T_C$  in the thermodynamic limit. At the

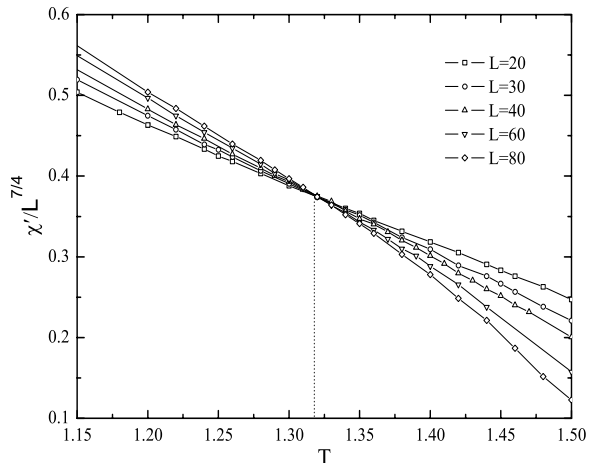


FIG. 2: Application of the finite-size scaling of in-plane susceptibility to estimate the phase transition temperature for  $\rho = 0.05$ .

phase transition temperature,  $U_L$  is expected to be approximately independent of the system size. Therefore,  $T_C$  can be obtained from the crossing point of  $U_L$  for different lattice sizes. As an example, Fig. 1 shows  $U_L$  for different lattice sizes at  $\rho = 0.05$ . The phase transition temperature is estimated at  $T_C = 1.328 \pm 0.002$ . Generally speaking, this method overestimates  $T_C$ . With increasing  $L$ , the estimation of  $T_C$  will be more accurate. Due to the statistical uncertainties, however, more computing time is required to calculate near  $T_C$ , especially in this model with nonmagnetic impurities.

Another method to estimate  $T_C$  proved to be very useful in many references [5, 6, 16, 17]. This method starts from the finite-size scaling analysis of the in-plane susceptibility  $\chi'$ . Near and below  $T_C$ , the susceptibility scales with a power of the lattice size,  $\chi' \propto L^{2-\eta}$ , even in the presence of nonmagnetic impurities. The critical exponent is  $\eta = 1/4$  at the BKT phase transition temperature for the planar rotator model and XY model. Therefore, using  $\eta = 1/4$ , from the common point of intersection of the curves  $\chi'/L^{7/4}$  vs  $T$ , the phase transition temperature can be obtained. Fig. 2 shows the application of this method at  $\rho = 0.05$ . The estimation of  $T_C$  is

$1.316 \pm 0.003$ , a little lower than the result from  $U_L$ .

In our practical application for this model, the statistical errors become even greater with the increase of  $\rho$ . More MC steps and averages are needed to reduce the errors when  $\rho$  increases, especially near the site percolation threshold  $p_c = 0.5$ . Therefore, using the largest lattice, we get  $T_C$  at high nonmagnetic impurity density based on the calculation of the helicity modulus.

The helicity modulus,  $\Upsilon$ , obtained by a measure of the resistance to an infinitesimal spin twist  $\Delta$  across the sys-

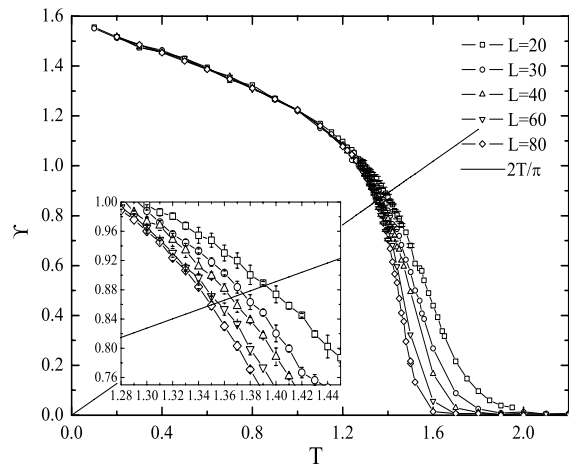


FIG. 3: Helicity modulus as a function of temperature for several lattice sizes at  $\rho = 0.05$ . The inset shows the view near the estimated critical temperature.

tem along one coordinate, is an efficient method to calculate the BKT phase transition temperature [18-20]. An expression applicable to any general model Hamiltonian is [6]

$$\Upsilon = \frac{\langle \partial^2 H / \partial \Delta^2 \rangle}{N} - \beta \frac{\langle (\frac{\partial H}{\partial \Delta})^2 \rangle - \langle \frac{\partial H}{\partial \Delta} \rangle^2}{N}, \quad (6)$$

where  $\beta = (k_B T)^{-1}$  is the inverse temperature. For the dilute planar rotator model, defined by equation (1), based on the derivation process of Ref. [21], we can get the expression of helicity modulus on the triangular lattice

$$\Upsilon(T) = -\frac{\langle H \rangle}{\sqrt{3}N_{mag}} - \frac{2J^2}{\sqrt{3}k_B T N_{mag}^2} \langle [\sum_{\langle i,j \rangle} (\hat{e}_{ij} \cdot \hat{x}) \sigma_i \sigma_j \sin(\theta_i - \theta_j)]^2 \rangle. \quad (7)$$

Here  $\hat{e}_{ij}$  is the unit vector pointing from site  $j$  to site  $i$ .  $\hat{x}$

is a selected basis vector in one coordinate. According to

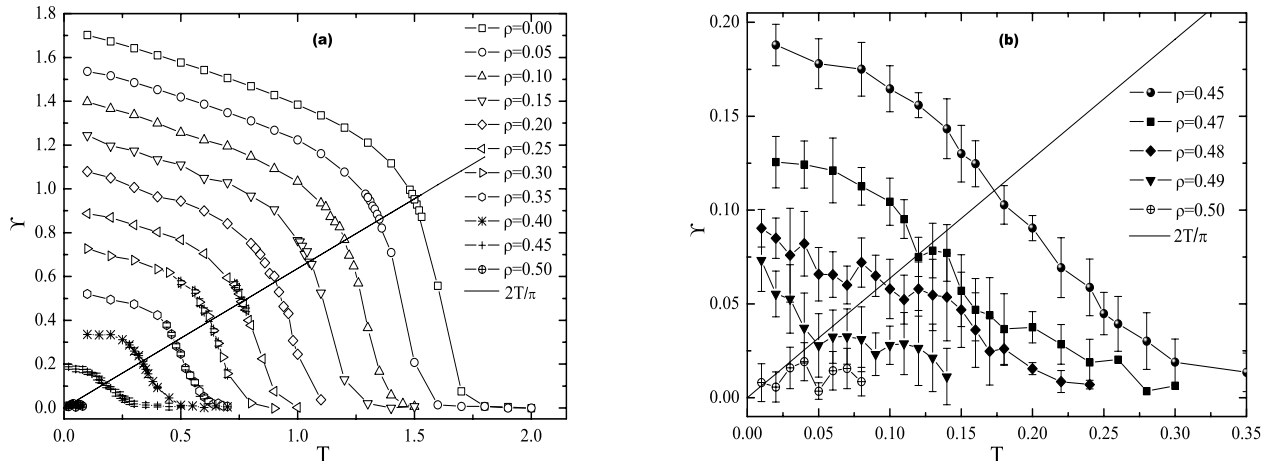


FIG. 4: Helicity modulus as a function of temperature for lattice size  $L = 80$  at different nonmagnetic impurity densities  $\rho$ . The overall trend and the results near the percolation threshold are shown in (a) and (b) separately.

the renormalization group theory [2], there is a universal relation between the helicity modulus and the phase transition temperature.  $T_C$  can be estimated from the intersection of the helicity modulus  $\Upsilon(T)$  and the straight line  $\Upsilon = 2k_B T/\pi$ . Meanwhile, the MC data of  $\Upsilon(T)$  will have a deeper drop in the critical region with increased lattice size. For larger lattice size, the intersection will be nearer to the critical temperature. Therefore, an overestimate of  $T_C$  generally will be obtained by this method. As an example, Fig. 3 shows the results for different lattice sizes at  $\rho = 0.05$ . It is clear that a BKT phase transition exists at finite temperature in this model. From the largest lattice size  $L = 80$ , we estimate the critical temperature  $T_C = 1.349 \pm 0.002$ , a little higher than that from the in-plane susceptibility  $\chi'$ . But that is to be expected, and only by going to much higher lattice size will the helicity-based approach give results that agree with those based on the susceptibility. It is noted that there is a greater statistical fluctuations at smaller  $L$ , while the statistical errors are almost smoothed out at large size. The helicity modulus for different  $\rho$  at  $L = 80$  is shown in Fig.4(a) and Fig.4(b).

Due to the critical slowing down at low temperature, it is clearly seen that the statistical errors are greatest when the magnetic occupation density  $\rho_{mag}$  is near  $p_c$ , where there is no spanning cluster to appear. The helicity modulus almost disappears at  $\rho = 0.50$ , as shown in Fig.4. As a comparison, for example, Fig.5 shows the results of finite-size scaling of in-plane susceptibility at  $\rho = 0.45$ . The statistical errors at small  $L$  are clearly more obvious than those at large  $L$ . The estimated phase temperature is  $T_C = 0.126 \pm 0.01$ , which is comparable with the result of helicity modulus as shown in Fig.4. The last results for phase transition temperature from the different methods

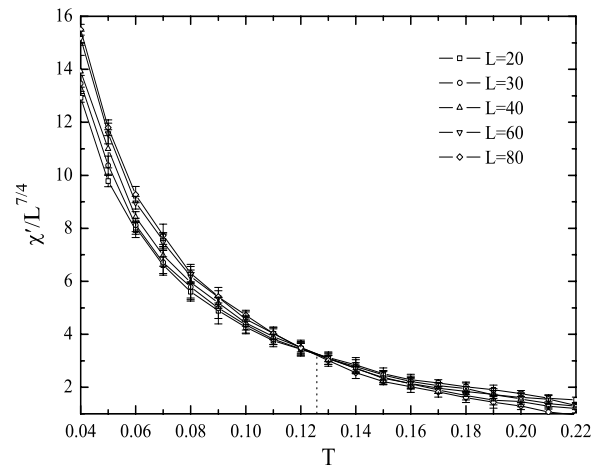


FIG. 5: Application of the finite-size scaling of in-plane susceptibility to estimate the phase transition temperature for  $\rho = 0.45$ .

mentioned above are summarized for different  $\rho$  in Fig. 6. We find that  $T_C$  is nearly linear with  $\rho$  and decreases with the increase of  $\rho$ . According to the linear fit of  $T_C$  from  $\Upsilon$ , we find that the BKT phase transition temperature falls to zero near  $\rho = 0.498 \pm 0.003$ , almost the same as expected from the site percolation threshold  $p_c = 0.5$ . This shows that the BKT phase transition vanishes when the magnetic site occupancy  $1 - \rho$  reaches the triangular lattice percolation limit, the same result as obtained for

this model on a square lattice.

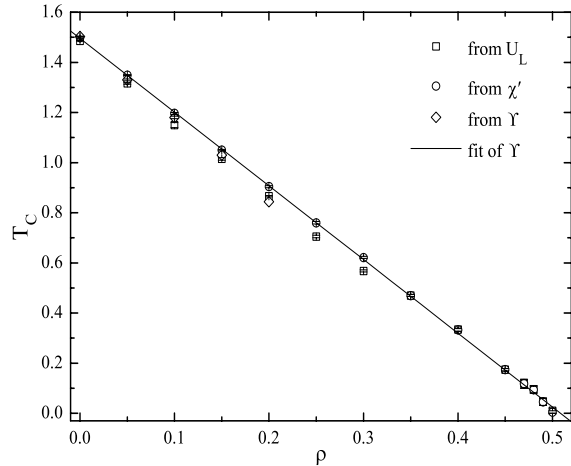


FIG. 6: Phase transition temperature estimated by the three methods for different nonmagnetic impurity densities  $\rho$ . The straight line is a linear fit to  $T_C$  obtained from the helicity modulus.

### III. CONCLUSIONS

In summary, with the application of a hybrid MC simulation, the BKT phase transition temperatures of a dilute planar rotator model on a triangular lattice are obtained by three methods. For the *pure* planar rotator model

( $\rho = 0$ ) on a triangular lattice as a test case, the phase transition temperatures we obtained from  $\chi'$ ,  $\Upsilon$  and  $U_L$  are  $1.486 \pm 0.002$ ,  $1.498 \pm 0.003$  and  $1.503 \pm 0.002$ , respectively. These data are comparable with the result of high-temperature series studies [22, 23]. Consistent with MC simulations on the square lattice [6], it is found that the phase transition temperature decreases as nonmagnetic impurity density  $\rho$  increases, and falls to zero only when the magnetic occupancy falls to the site percolation limit. This is completely reasonable, considering that the correlation length could not diverge and hence there would be no BKT phase transition if there were no percolating cluster spanning the system. On the other hand, as long as any percolating cluster is present, the BKT phase transition should appear, but at a reduced temperature due to the diluted effective exchange couplings between distant spins. Meanwhile, we find there is close to a linear relation between  $T_C$  and  $\rho$ . Stated simply, the BKT phase transition is present only when  $\rho_{mag} > p_c$ , and the phase transition temperature is approximately linearly proportional to  $(\rho_{mag} - p_c)/(1 - p_c)$ . The calculations become more difficult when the magnetic density is close to the percolation limit, due to the combined BKT and percolation fluctuations there. Thus, we could not rule out a weak deviation from this linear relationship when  $\rho_{mag}$  is very close to  $p_c$ .

### Acknowledgments

This work was supported by the National Natural Science Foundation of China under Grants No. 10774053 and the Natural Science Foundation of Hubei Province under Grants No. 2007ABA035.

- 
- [1] V.L. Berezinskii, Sov. Phys. JETP **34**, 610 (1972).
  - [2] J.M. Kosterlitz, D.J. Thouless, J. Phys. C **6**, 1181 (1973).
  - [3] S.A. Leonel, P. Zimmermann Coura, A.R. Pereira, L.A.S. Mól, and B.V. Costa, Phys. Rev. B **67**, 104426 (2003).
  - [4] B. Berche, A.I. Fariñas-Sánchez, Yu. Holovatch, and R. Paredes V, Eur. Phys. J. B **36**, 91 (2003).
  - [5] G. M. Wysin, Phys. Rev. B **71**, 094423 (2005).
  - [6] G. M. Wysin, A. R. Pereira, I.A. Marques, S.A. Leonel, and P.Z. Coura, Phys. Rev. B **72**, 094418 (2005).
  - [7] L.M. Castro, A.S.T. Pires, and J.A. Plascak, J. Magn. Mater. **248**, 62 (2002).
  - [8] Y.E. Lozovick, L.M. Pomirchi, Phys. Solid. State. **35**, 1248 (1993).
  - [9] M.F. Sykes, J.W. Essam, J. Math. Phys. **5**, 1117 (1964).
  - [10] P.W. Leung, C.L. Henley, Phys. Rev. B **43**, 752 (1991).
  - [11] N. Metropolis, A.W. Rosenbluth, M.N. Rosenbluth, A.H. Teller, and E. Teller, J. Chem. Phys. **21**, 1087 (1953).
  - [12] F.R. Brown, T.J. Woch, Phys. Rev. Lett. **58**, 2394 (1987).
  - [13] M. Creutz, Phys. Rev. D **36**, 515 (1987).
  - [14] U. Wolff, Phys. Rev. Lett. **62**, 361 (1989).
  - [15] K. Binder, Z. Phys. B: Condens. Matter. **43**, 119 (1981).
  - [16] A. Cuccoli, V. Tognetti, R. Vaia, Phys. Rev. B **52**, 10221 (1995).
  - [17] L.A.S. Mól, A.R. Pereira, H. Chamati and S. Romano, Eur. Phys. J. B **50**, 541 (2006).
  - [18] H. Weber, P. Minnhagen, Phys. Rev. B **37**, 5986 (1988).
  - [19] Y.H. Li, S. Teitel, Phys. Rev. B **40**, 9122 (1989).
  - [20] P. Olsson, Phys. Rev. Lett. **75**, 2758 (1995).
  - [21] D.H. Lee, J.D. Joannopoulos, J.W. Negele, and D.P. Landau, Phys. Rev. B **33**, 450 (1986).
  - [22] M. Ferer, M.J. Velgakis, Phys. Rev. B **27**, 314 (1983).
  - [23] P. Butera, M. Comi, Phys. Rev. B **50**, 3052 (1994).